

Statistical Instability of the Ramp Discharge and the Role of Exoemission.

V. P. Nagorny, V. N. Khudik

*Plasma Dynamics Corporation, Waterville, OH 43566 **

A. Shvydky

University of Toledo, Toledo, OH 43606

Dynamics of the ramp discharge is studied via kinetic PIC/MC simulations. It is shown that pdp cell is fundamentally "small" system and fluctuations of the number of charged particles in the discharge gap strongly influence the dynamics of the ramp discharge and may even lead to its disruption. Common view of ramps based on multi-cell or time averaged measurements, and corresponding fluid theoretical descriptions are inadequate. The role of exoemission as a possible stabilizer of the discharge is clarified.

Keywords: plasma display, ramp discharge, dielectric barrier discharge, Townsend discharge, fluctuations

I. INTRODUCTION

Ramp discharge [1] is currently widely used in plasma displays during the display setup period, when all cells independently of their initial wall charges are set to a specific state, convenient for addressing. The basic idea behind the ramp is shown in Figure 1. When one slowly increases the voltage across a cell's gap from a low value, there is no discharge activity in the cell until the gap voltage reaches the breakdown voltage V_b for that particular cell. As soon as the gap voltage exceeds V_b , the cell becomes active and the voltage across the gap stays constant, and equal to V_b . As the ramp voltage V_{appl} progresses, every cell will eventually discharge with their respective V_b values appropriate for each individual cell. If after a while, as shown in Fig. 1 one starts to ramp the voltage down, then discharge stops and starts again when the voltage across the gap reaches the value V_b , but in the opposite direction. As it was during the ramping up, the voltage across the gap stays equal to V_b . If at some point ($t = 1100\mu s$ in the Fig. 1), one stops the ramp and raises the applied voltage by, say $20V$, then every cell is left $20V$ below the breakdown voltage independently of the value of the breakdown voltage of that particular cell, and of the initial wall voltage (V_W) at $t = 0$. Such exact setting of the wall voltage during the setup is very valuable, because it allows one to use relatively low voltages for the selective addressing operation since no excess voltage is needed to cover any possible uncertainty in wall voltages.

Later we developed a theory of the ramp discharge [2], based on the hydrodynamic approximation, which is supported by numerous experiments and simulations [3–7]. This theory (see Appendix) shows that in most cases voltage across the gap oscillates around the breakdown voltage, rather than stays constant. The stationary conditions in the ramp discharge (voltage, current, electron and ion densities) are achieved as a result of the balance

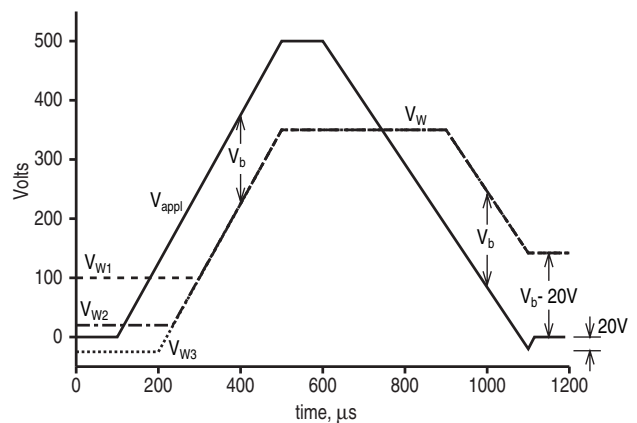


FIG. 1: The applied voltage V_{appl} and wall voltages V_W for three different initial wall voltages during the setup period. There is no discharge activity in the cell until the gap voltage reaches the breakdown voltage V_b for that particular cell. As soon as the gap voltage exceeds V_b , the cell becomes active and the voltage across the gap stays constant, and equal to $\pm V_b$.

between ion losses to the cathode and their production in the avalanches started by secondary electrons. This balance is described by the Townsend condition:

$$\gamma(e^{\alpha L} - 1) = 1. \quad (1)$$

Here γ is the secondary electron emission coefficient, describing the number of electrons (avalanches) that start from the cathode per incident ion, α - is the first Townsend coefficient, L is the gap length and the factor $(e^{\alpha L} - 1)$ describes the number of ions produced in the avalanche initiated by one secondary electron. Thus, the production $\gamma(e^{\alpha L} - 1)$ shows the number of ions produced in the gap per one ion lost at the cathode. If this production is equal to one (as in Eq. (1)), then every ion lost at the cathode is replaced by exactly one ion produced in the gap, and their density stays constant. Electric field (voltage) is included in Eq. (1) through the first Townsend coefficient (α), which grows with electric

*Electronic address: vnagorny@plasmadynamics.com

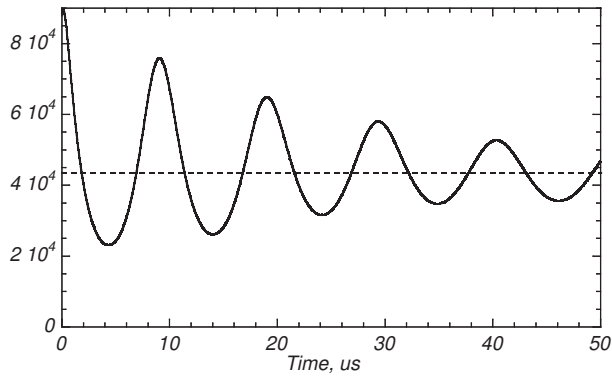


FIG. 2: Typical behavior of the ion number in a cell during the ramp with good initial conditions (3D Fluid simulations). The dashed line shows the number of ions related to a steady current, without oscillations.

field.

Oscillations of the ion density and current during the ramp appear when initial ion density is lower, or higher than the one required to sustain the current CdV_{appl}/dt , where C is the capacitance of the dielectric, when the voltage across the gap is equal to V_b . Let's say the ion density at this moment is low, then when the voltage across the gap (during the ramp) exceeds the breakdown voltage, the left side of the Eq. (1) is larger than 1, and the ion density grows - discharge strengthens. The wall charge, deposited on the electrodes in the result of this discharge, is large enough to put the resulting voltage across the gap below the breakdown value. From this moment the discharge weakens, until the voltage across the gap rises again above the breakdown one (due to the ramp), then the next discharge starts, and so on. The better initial conditions in the gap, the closer they to the ideal ones (those that produce stationary current without oscillations), the smaller oscillations of the current, ion density, and the voltage across the gap. Too high, or too low initial density causes large oscillations. Based on this theory, if initial conditions are good, and the ramp rate is not too high, then the ramp will be stable.

In a real cell with three or more electrodes, a single breakdown voltage has to be replaced by a set of voltages (the VT-curve [8, 9]), oscillations have a more complicated structure, and may decay, as in Figure 2, even when they are not decaying in the 1D model, but their mechanism is still the same as we described above.

In this paper we point to a new feature, specific for plasma display panels (PDPs). Due to a small size of a PDP cell ($\sim 10^{-5}cm^3$) the number of charged particles participating in the ramp discharge in any individual cell is relatively small - some tens of thousands of particles. This causes emerging of new kind of effects - statistical ones, which fluid approximation, and even kinetic Boltzmann approach completely ignore. On the other hand, because of a small number of particles these effects can be very efficiently investigated using Monte-Carlo approach.

As it turned out, they are indeed very important, especially for low ramp rates, and mixtures with high concentration of Xe. We discovered that for conditions of the ramp discharge in a PDP cell statistical fluctuations of the number of ions in the gap N_i (and current) are very large, they lead to instability of the ramp discharge, and eventually to complete loss of charged particles from the discharge gap. Opposite to a large size discharge, where the number of ions in the gap can easily be of the order of $10^8 - 10^{10}$, the initial density of charged particles plays much less important role in a microdischarge, but the role of independent sources, like exoemission, in stabilizing discharge increases very much.

The statistical instability behaves not like a regular instability, where a small initial fluctuation grows exponentially with time. Instead, every fluctuation here does not grow, but changes the discharge conditions leading to oscillations of the current, and ion density. The series of uncorrelated fluctuations leads to large oscillations, and ultimately to complete extinguishing of the discharge. The time for such disruption depends on the average current, initial conditions and a specific sequence of random collisions - discharge may die right away, or after many oscillations.

The plan of this paper is as following. In Section II we present the results of 3D kinetic (PIC/MC) simulations of the ramp discharge in a PDP cell and in a special test cell, and analyze them. In Section III we show that exoemission may stabilize the discharge. Finally, in the Section IV we make summation remarks.

II. 3D MONTE-CARLO SIMULATIONS OF THE RAMP

As we mentioned above, fluid approximation is applicable when the number of particles is very large, and statistical fluctuations are negligibly small. On the other hand, when the effective secondary emission coefficient γ is small, the average number of ions in the cell during the ramp discharge is about

$$\langle N_i \rangle \approx (\tau_i/2e)CdV_{appl}/dt, \quad (2)$$

where τ_i is the ion transit time across the gap. For typical parameters of the PDP cell ($C \sim 0.02pF$, and $\tau_i \sim 100ns$) it gives $\langle N_i \rangle \sim 10000 - 40000$. During the ramp oscillations (as in Fig. 2), N_i can become even lower, and fluctuations may become very important. In this case one can only use a Monte-Carlo approach - the only kinetic approach which properly takes into account the statistical nature of the processes responsible for production of charged particles in the gap (secondary electron emission and ionization).

As one can see from the Fig. 3, which shows the total number of ions in the same PDP cell driven with the same ramp rate obtained in 3D fluid and 3D PIC/Monte-Carlo simulations, fluctuations indeed change the discharge behavior dramatically. Both ramps started at $t = 0$ with

the same wall charge distribution obtained in 3D fluid simulation of the sustain discharge, the same number of ions in the gap and the same (close to the breakdown) voltage. Initial particle distribution in the kinetic simulation was close to that in the fluid one. While amplitude of the oscillations in the kinetic simulation in the beginning of the ramp is smaller than that in the fluid one, the kinetic simulations show emerging of large oscillations of the number of ions in the cell and even disruption of the discharge, in contrast to fluid simulation, which show regular, slow decaying oscillations (some increase of the oscillations around $t = 45\mu s$ is caused by the initiation of the second discharge between sustain and data electrodes).

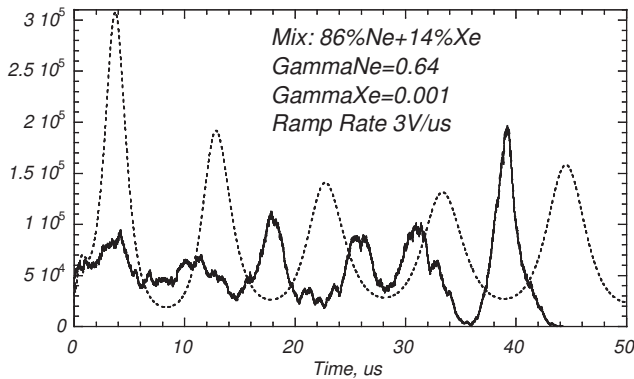


FIG. 3: Total number of ions calculated for identical ramps in identical cells. While fluid simulations (dashed line) show regular decay of oscillations, kinetic simulations (solid line) show irregular behavior, caused by fluctuations, and finally discharge died at 40mks. The increase of the current in fluid simulation is caused by initiation of the second discharge.

To separate statistical effects from the geometrical ones, we start our analysis with a 1D ramp investigation, where the electric field has only one component, but particles can move in all directions. For this reason we consider discharge in the test cell with reflective sidewalls parallel to the electric field. The transverse dimensions of the cell are $100\mu m \times 100\mu m$, the gap $(90 - 100)\mu m$ and the capacitance of the dielectric covering electrodes varies in the range of $0.016 - 0.064 pF$. We start all ramps at $t = 0$ with the voltage equal (or close) to the breakdown voltage, placing in the gap the number of ions close to the one given by Eq.(2)(and appropriate number of electrons), and distributed in a way that would produce stationary discharge according to the fluid theory. One should note, though, that because of a small ion transit time compared to the period of oscillations (see Appendix), any other initial profile would result in a some noise lasting for just a few ion transit times, but will not lead to large, long period oscillations. In the absence of fluctuations the initial conditions we have chosen would result in small weakly decaying oscillations, so one can assume that any difference in the discharge behavior is caused by fluctuations.

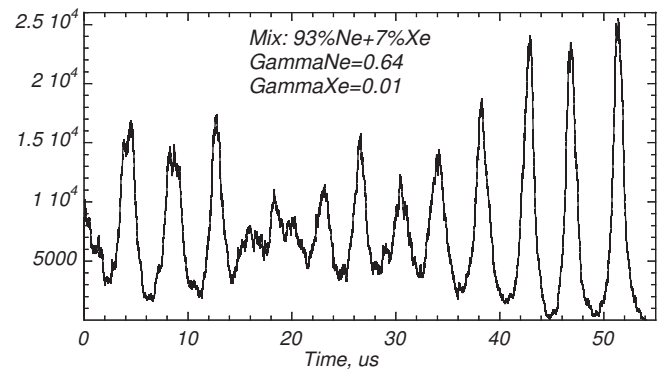


FIG. 4: Ramp discharge starts with "ideal" initial conditions. Ramp rate is $4.2V/\mu s$, dielectric capacitance is $1.6pF$. Fluctuations are responsible for initial deviation from the ideal conditions in the gap, and for the successive variations of the amplitude of the oscillations. If at any moment Monte-Carlo simulations were replaced by fluid simulations, they would show a steady, slow decaying oscillations from that moment on.

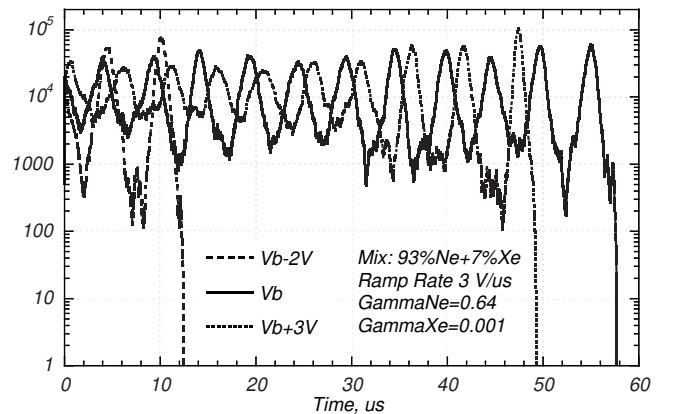


FIG. 5: Total number of ions N_i in the gap during the ramp discharges started with voltages close to V_b , and initial number of particles close to the one given by Eq. (2) (≈ 18000). Oscillations of N_i show large fluctuations around minimums and eventually complete loss of particles.

Figure 4 shows the number of ions in the gap in the ramp discharge started at almost ideal initial conditions ($V = V_b$, $N_i = \langle N_i \rangle$, V - voltage across the gap). One can see that there is no regularity in the variation of the **amplitude** of oscillations. It increases or decreases, depending on the sequence and the magnitude of fluctuations rather than on macroscopic discharge conditions. At some point ($t \approx 20\mu s$) oscillations disappear and then reappear until large oscillation occurs and discharge ends, at $t \approx 54\mu s$. Opposite to the fluid theory, which predicts constant number of ions for such initial conditions, not only oscillations have appeared, but the number of ions in the gap oscillated until they completely disappeared.

Fig. 5 shows three ramp discharges - all started around

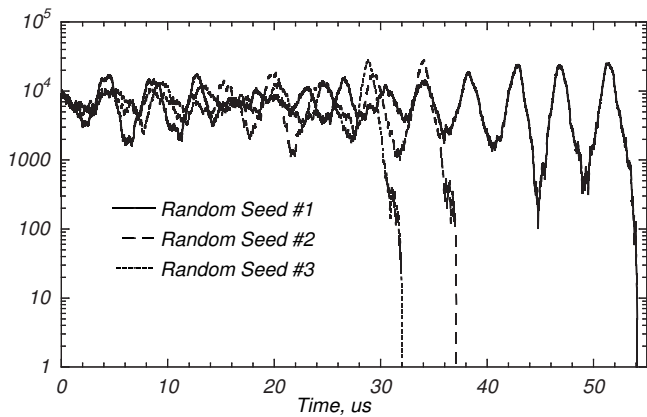


FIG. 6: Three ramp discharges start with identical macroscopic initial conditions - same as in discharge shown in the Fig. 4. They only have different sequences of random numbers, generated by the same random numbers generator. These random numbers control the specific order of microscopic events - secondary electron emission and collisions.

the breakdown voltage with the same number of injected particles. All of these discharges demonstrate irregular fluctuations of the amplitude of the oscillations and finally the complete disruption of the discharge. One can see that the discharge "lifetime" - changes dramatically with initial voltage. One should remember though, that it is incorrect to speak of a certain discharge "lifetime" in the presence of large fluctuations. Discharge could easily die near any of the minimums of the ions density.

Single simulation can only show how ONE cell will behave in ONE ramp. The other (identical) cell or the same cell in a different ramp may behave quite differently. Discharge may be much longer or shorter, with smaller or larger oscillations. But the fact is: large oscillations will necessarily appear, and sooner or later discharge dies. Figure 6 shows three "would be" identical discharges (one is the same as in the Fig.4), the only difference between which is the different sequences of random events, controlled by the "seed" number of the random number generator. These sequences describe actual random events like secondary emission or ionization processes. For example, for the fluid consideration the secondary emission coefficient $\gamma = 0.01$ means that electron flux from the cathode is at all times a hundred times smaller than the ion flux to it, independently on how many actual ions arrive to it. In the Monte-Carlo consideration (as in real life), when ion arrives to the surface, it does not produce 0.01 electron. This coefficient γ describes only the probability of the electron emission. Actual electron may be emitted after first, twenty first or two hundredth ion arriving to that surface. Similar probability consideration applies to the excitation and ionization events.

The comprehensive theory showing how seemingly small fluctuations can lead to such a dramatic effect as a discharge disruption, is beyond the scope of this pa-

per and will be published later. Here we explain this effect qualitatively. We will show first that for the typical conditions of a PDP ramp discharge these fluctuations are not small at all. Since particles practically do not affect the electric field in the gap, and the characteristic time of the macroscopic changes is large compared to the ion transit time [10] one can analyze fluctuations (and the dynamics of the discharge) in terms of the number of particles in subsequent generations. Ideally, the number of ions in the gap stays constant, equal to $\langle N_i \rangle$, Eq. (2), which is provided by the balance between secondary emission (γ) and amplification in the avalanche ($\sim \exp(\alpha L) \sim 1/\gamma$). In reality both processes have statistical nature, which means that the number of secondary electrons emitted from the surface is not exactly γN_i , but has fluctuations with dispersion of the order of $\sqrt{\gamma N_i}$ (when N_i is large). After the avalanche with amplification factor $\sim 1/\gamma$, the number of ions in the gap differs from the original one by $\delta N_i \sim \sqrt{N_i/\gamma}$. The second statistical process is the multiplication in the electron avalanche. Simulations show that fluctuations due to this process have the same order of magnitude $\delta N_i \sim (1/2) \exp(\alpha L) \sqrt{\gamma N_i} \sim \sqrt{N_i/\gamma}$. This result explains why the role of fluctuations is so significant - the relative fluctuations $\delta N_i/N_i \sim 1/\sqrt{\gamma N_i}$ are small only when $N_i \gamma \gg 1$, which is much more restrictive than $N_i \gg 1$, and $\delta N_i/N_i$ can easily be about 0.1-1 in the minimums of the current oscillations, if γ is small enough. For example, for the typical ramp rate of $3V/\mu s$, one requires about $N_i \sim 20000$ ions in the gap to sustain the current in the "test" cell. With effective secondary emission coefficient γ of 0.5 the deviation of ions in the gap from one generation to another is about $\delta N_i \sim (N_i/\gamma)^{1/2} \sim 200$, which is about 1% of the total number of ions. On the other hand, for more realistic $\gamma \sim 0.005$, $\delta N_i \sim 2000$, or 10%. In deep minimums relative fluctuations are even larger. The dependence of the amplitude of fluctuations on γ is illustrated in Fig. 7, which shows two discharges in the 93%Ne + 7%Xe mixtures, where two different values for the xenon secondary emission coefficient has been used. Oscillations are being observed in both of these cases, but in the case of large γ they seemed to be bound within some limits. Since effective γ depends on the gas mixture, one should expect larger fluctuations in mixtures with larger xenon component, where effective γ is very small. The above consideration shows that PDP ramp discharge may have large statistical fluctuations even when the number of particles participated in it is large (tens of thousands), especially when mixtures with large xenon component are used.

Obviously, when the number of ions in the gap becomes small ($(N_i \gamma)^{1/2} \sim 1$), and relative fluctuations ($\delta N_i/N_i$) increase, then just a few fluctuations may end the discharge, and in many cases this is exactly what happens. In other cases fluctuations cancel each other or lead to an increase of the number of particles, so that the discharge recovers (current rises), but near every minimum the probability of the discharge to end grows up again,

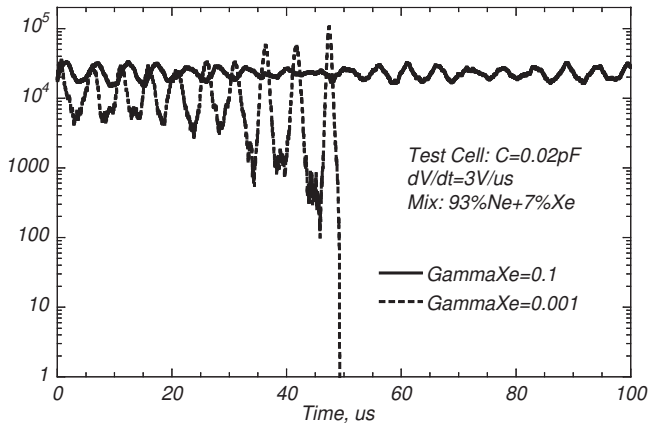


FIG. 7: Both discharges start with "ideal" initial conditions, and have $\langle N_i \rangle \approx 20000$. Discharge with small γ_{Xe} demonstrate much larger fluctuation, and oscillations. In both cases the vacuum value of γ_{Ne} is 0.64.

and in one of them it dies.

The initial oscillations of the current come either from initial conditions, or again from the fluctuations, which easily take the system far off the balance (Eq.(1)) since the "feedback" at this point ($V = V_b$) is weak. As oscillations become larger, fluctuations with larger magnitude occur, and they may take the system even further off the balance. This makes the ramp discharge unstable toward disruption. As we already mentioned before, unlike a regular instability, where any initial perturbation only grows, here fluctuations do not grow, but the high probability for a sequence of fluctuations to end the discharge makes it unsustainable.

The described mechanism of the ramp instability is quite powerful and works even if the number of particles $\langle N_i \rangle$ is large or the effective secondary electron emission coefficient γ is not very small. Although discharge lifetime may become quite long, for the ramp setup to work, it is necessary that discharges **in each** of millions of cells of the panel during each of millions of reset ramps were stable and not disrupted, otherwise some cells will be misaddressed.

III. STABILIZING THE RAMP. EXOEMISSION

As we have shown in the previous Section, the PDP ramp discharge is not sustainable. When no charged particles are left in the cell, the only way to restart discharge again and to continue the ramp is through additional independent source of electrons, or ions. The most important of such external sources is electron exoemission [11–14], because it decays much slower than others, and thus is the only one that can again initiate the discharge. Indeed, those cells that were not lit during the subfield preceding the ramp, were losing both charged and excited particles for at least $1ms$ - particles one needs to start

the discharge, when the ramp voltage is applied. For the neon and xenon mixture the slowest decaying species are xenon metastables ($Xe^*(^3P_2)$), since they are not affected by electric field, and do not radiate. However, due to collisions with the background gas metastables can form an excited xenon molecule, Xe_2^* , which quickly radiates. The decay of the number of metastables is thus controlled by the conversion rate of $Xe^*(^3P_2)$ to $Xe_2^*(^3\Sigma)$ in the reaction $Xe^*(^3P_2) + Xe + M \rightarrow Xe_2^*(^3\Sigma) + M$, where Xe denotes the xenon atom and M can be either xenon or neon atom of the background gas. The rate of this reaction (in s^{-1}) is about $1/\tau_{conv} \sim 15p^2\xi(1+3.6\xi)$, where p is the gas pressure in Torr, and ξ is the ratio of xenon partial pressure to the total pressure ($\xi = p_{Xe}/p$). For typical gas pressure of about $500Torr$, and $\xi \sim 0.05$, the conversion time τ_{conv} is only about $4.5\mu s$, and is even smaller for the mixtures with larger xenon component. So if the peak number of metastables in a cell during sustain period is even about $N_m \sim 10^9 - 10^{10}$, then it will take only about $\tau_{conv} \ln N_m \sim (90 - 100)\mu s$ for all of them to completely disappear.

So, the only source of electrons in the cell that can work for a long time (much longer than $1ms$) is electron exoemission [11–14] from MgO surface, excited by electrons, ions and photons during sustain period. Every two sustain pulses about 10^8 electrons and ions strike MgO surface just above sustain electrodes, filling the energy levels in the forbidden zone, and making holes in the valence band. As electrons and holes recombine in the process of MgO relaxation, the released energy may be absorbed by another electron trapped in the forbidden zone, which may be ejected from the surface. The exoemission rate depends on the number and distribution of energy levels in the forbidden zone, the number of electrons in the forbidden and conductive bands and holes in the valence band, temperature, etc., which should be a subject of a separate investigation. In this paper we will simply use the fact that this process exists and investigate its effect on the ramp. It is imitated by a random emission of electrons (with specified average rate) from a random position on the cathode surface.

While in all our simulations described in the previous section, we have used "good" initial conditions, when one could expect that fluctuations are small at least in the beginning of the discharge, for the real panel conditions one should expect only a few (if any) electrons or ions in the gap, and since the point of this Section is to show the possible stabilization of the ramp, we start all simulations assuming that there are no charged particles in the volume (at $t = 0$).

Obviously, if exoemission is weak, then discharge may actually die, then start again, then die, etc. (see Fig. 8a). In this case discharge may have very large peaks, and the voltage across the gap before and after peak may differ by $10 - 20V$. Finally, if exoemission is strong, then the ramp is stable. One should remember though, that if exoemission is too high, then the voltage across the gap is stabilized at the level below the breakdown, and that

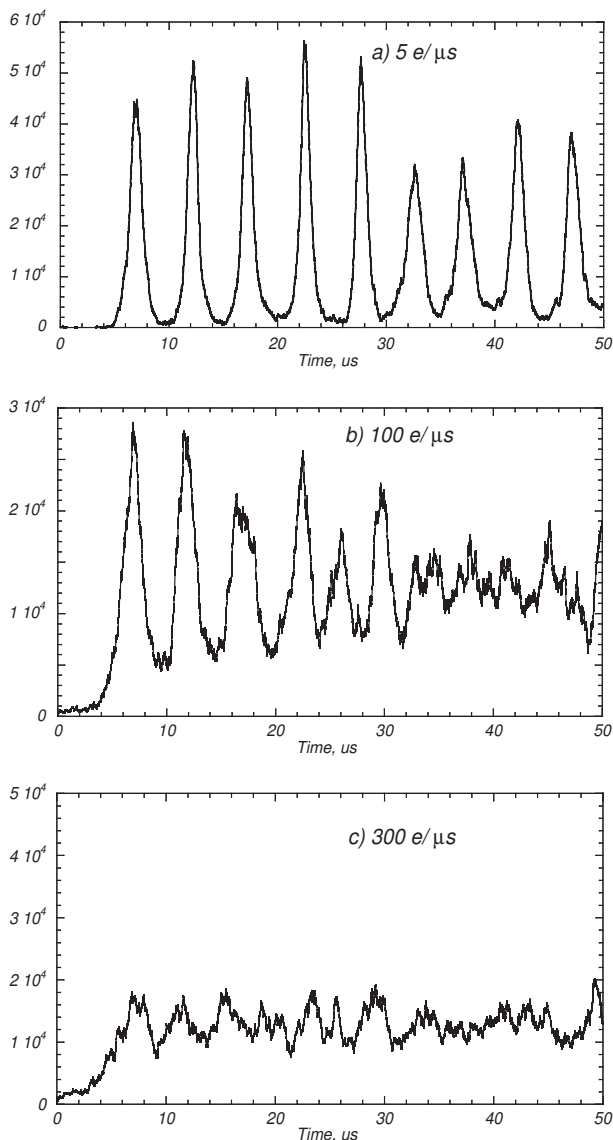


FIG. 8: 1D Monte-Carlo simulations of the exoemission in the "test" cell. We choose 93% Ne + 7% Xe mixture and for comparison with previous results. Low exoemission rate results in many separate, not sustainable discharges, some of which are very strong. With increasing the exoemission rate, oscillations of the ion density decrease, and discharge becomes stable. Initially, no charged particles are assumed in the gap.

after the ramp exoemission continue to "work", so one has to take special measures to save the wall charge.

The plots of the ion density during the ramps in the 1D test cell and in the 3D pdp cell - the same that we have used in the simulations shown in the Fig. 3, but in the presence of the exoemission from the cathode are shown in the Figs. 8- 9. We started every simulation with no charged particles in the volume, and chose the ramp rate of $3V/\mu s$. We used mixture of 93% Ne + 7% Xe for the test cell and 86% Ne + 14% Xe for the pdp cell, and assumed that $\gamma_{Xe} = 0.001$ - the case that would certainly

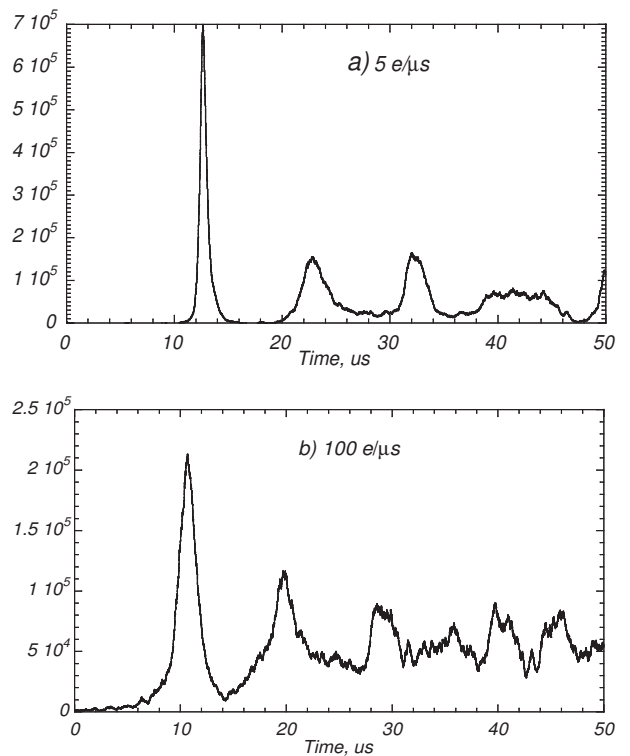


FIG. 9: 3D Monte-Carlo kinetic simulation of the ramp in the pdp cell with 86% Ne + 14% Xe mixture. Low exoemission results in a separate peaks. Higher exoemission provides stability, although some noise is present.

be unstable without exoemission. The initial voltage was chosen slightly below the breakdown voltage, so until the voltage across the gap exceeded V_b the number of ions in the gap stayed too low to be seen in some of these figures.

For dimensions of the pdp cell we have used the following:

Cell Pitch - 675μ ,

Plate Gap (gap between dielectrics of the front and back plates)- 80μ ,

Sustain Gap (gap between sustain electrodes) - 100μ ,

Sustain electrode width - 90μ ,

Data (address) electrode width - 80μ ,

Dielectric thickness (front) - 25μ ,

Dielectric and phosphor thickness (back) - 25μ ,

Barrier rib pitch - 220μ ,

Barrier rib thickness - 40μ ,

Thickness of the phosphor layer - 10μ .

Our choice of γ_{Xe} is quite arbitrary, as it is not really known. Obviously, if we used larger γ_{Xe} , the required exoemission rate would be reduced. In both cells (test and pdp) the exoemission rate of 5 electrons per microsecond ($5e/\mu s$) from the cathode surface is not enough - oscillations are too large, but $100e/\mu s$ was good enough to stabilize the discharge (Figs. 8-9).

Simulations of longer ramps in different pdp cells and with different mixtures produce similar results. Higher

ramp rates result in more stable discharges, with a lower noise level.

IV. SUMMARY

It is generally assumed that individual cells are large enough, so that statistical effects are negligible, and it doesn't matter whether you investigate one or a hundred cells. Based on this view, investigators measure total current (light) from many cells [3], or considered data, accumulated over time. Interesting, that the origin of a very large noise of the IR signal, recorded from about 10000 cells [3], which should not be there if all cells worked according to a fluid theory, was never analyzed. Our investigation have shown that statistical effects in a **single cell are "large"** and that the multi-cell (or time-averaged) investigations of ramps are fundamentally inadequate, as they may show smooth stable current, masking effect that some of the cells may be unstable. In a way, averaged approach hides microscopic problems. While the fluid approximation (equivalence of the averaged approach) still being very good for investigating a discharge far from the breakdown, when one of the processes (production or losses of particles) strongly dominate the other one, it is never good for investigating a stationary ramp discharge (especially in a single cell), where the losses of the particles are compensated by the ionization in the avalanche from the secondary electrons. For the stationary ramp to exist, the delicate balance between amplification in the avalanche and the secondary emission should be provided. In reality, both secondary emission and particle amplification in the electron avalanche have statistical nature, and the statistical noise (which can be very large, especially when the secondary emission coefficient is small) will always bring the ramp off the balance, and finally discharge will die.

This conclusion contradicts to a common view that as long as the priming is good in the beginning of the ramp (i.e. the initial conditions are close to the "ideal" ones) it can be sustained and the oscillations of the ramp are initiated by the bad priming. Secondary sources, like exoemission were never considered to be important after the ramp started. As we have shown above, one should have a very significant secondary source during the whole length of the ramp in order to stabilize the ramp in mixtures with large xenon component. On the other hand the strong exoemission may be a problem when the OFF cell is being sustained - its wall charge can be partially erased, so one has to take a special care to avoid it.

We do not have any exoemission data and the secondary emission data are very unreliable. As a matter of fact, as far as we know, nobody have measured the secondary emission coefficient in the presence of exoemission. While exoemission itself does not affect secondary emission coefficient, the condition of the surface required for exoemission, may significantly increase the secondary emission coefficient. If so, then one may observe stable

ramps, even at relatively low exoemission levels.

These results show the importance of a **real time measurements on a single cell**. Since they differ so much from the common view, the determination of the correlation between stability of the ramp and exoemission level during and before the ramp and/or stability of the ramp and priming (when exoemission is suppressed) would be very important. The exoemission can be "stimulated" by using, for example, different temperatures or external UV source that would irradiate the cathode.

V. APPENDIX

Equations describing slow ($\tau \gg \tau_i$, [10]) variations of the current j and the voltage across the gap V during the ramp discharge, when V stays close to V_b , and the charged particles density in the gap is low so that they do not effect the electric field in the gap are (see [2]):

$$\frac{\partial j}{\partial t} = \frac{\kappa}{L}(V - V_b)j, \quad (3)$$

where $\kappa = \kappa(\alpha, \gamma, v_i, L) \approx Lv_i(\partial\alpha/\partial V)|_{V=V_b}$, $\alpha = \alpha(V/L)$ - is the first Townsend coefficient, L - the gap length, and

$$\frac{\partial V}{\partial t} = -C^{-1}(j - j_{DC}), \quad (4)$$

where C is the capacitance of the dielectric layers, $j_{DC} = CdV_{appl}/dt$, and V_{appl} is the applied voltage. The stationary solution of Eqs. (3-4) is obvious:

$$V = V_b, \quad j(t) = j_{DC}. \quad (5)$$

One can rewrite Eqs. (3-4) in the form of Hamilton's equations, for a particle of "mass" L/κ if we choose new variables "momentum" $P = V - V_b$, and "coordinate", $Q = \ln(j/j_{DC})$:

$$\dot{Q} = P/m = \frac{\kappa}{L}P = \frac{\partial H(P, Q)}{\partial P}, \quad (6)$$

$$\dot{P} = \lambda(1 - e^Q) = -\frac{\partial U}{\partial Q} = -\frac{\partial H(P, Q)}{\partial Q}, \quad (7)$$

where

$$H(P, Q) = P^2/2m + U(Q), \quad U(Q) = \lambda(e^Q - Q). \quad (8)$$

are the Hamiltonian of the system, and the "potential", and $\lambda = dV/dt$ is the ramp rate.

Equations (6-7) have the integral of "motion", equivalent to a particle energy

$$W = H(P, Q) = \kappa \frac{(V - V_b)^2}{2L} + \lambda(e^Q - Q) = const, \quad (9)$$

and since the potential (11) represents a well, the energy conservation describes periodic oscillations. Potential $U(Q)$, has its minimum value at $Q = 0$, so the

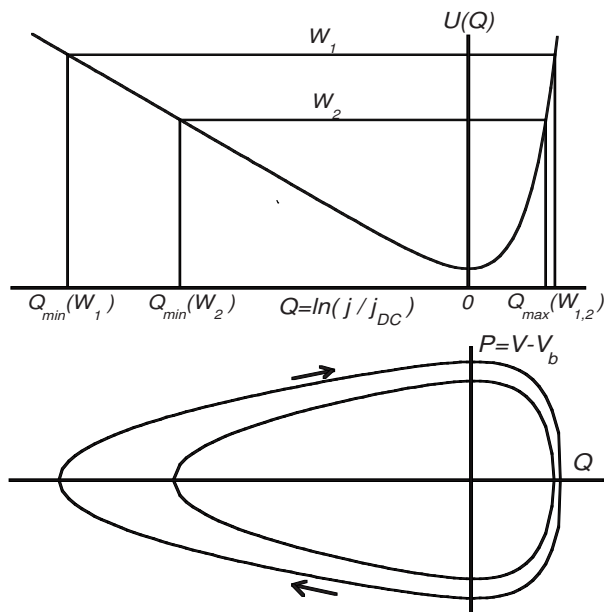


FIG. 10: Function $U(Q)$, and phase trajectories. Two horizontal lines show two different values of the energy $W = W_1$, $W = W_2$, $W_1 > W_2$. The larger oscillations of a current (higher peaks and lower deeps) correspond to the larger energy.

"particle" oscillates between points $Q_{min}(W) < 0$, and $Q_{max}(W) > 0$ (see Fig. 10). The period T of current

oscillations depends on their energy W :

$$T = \oint \frac{dQ}{\sqrt{(2\kappa/L)(W - U(Q))}}. \quad (10)$$

When oscillations are small they become harmonic ones of a frequency $\omega = \sqrt{\lambda\kappa/L} \sim \sqrt{v_i\lambda(\partial\alpha/\partial V)|_{V=V_b}}$. When oscillations are large, T is determined by the linear part of $U(Q)$ (when the current is small), and it increases with the amplitude of oscillations $T \sim 2\sqrt{2WL/\kappa/\lambda} \sim 2\sqrt{2L/(\kappa\lambda)}\sqrt{j_{max}/j_{DC}}$.

Both extremes are obviously occur at $P = 0$ ($V = V_b$), so with any priming ($Q(t = 0)$) oscillations smaller if $P(t = 0) = 0$, or $V(0) = V_b$. For large current oscillations ($\exp|Q_{max,min}| \gg |Q_{max,min}|$) we obtain $W = -\lambda Q_{min} = \lambda e^{Q_{max}}$, or

$$j_{max} = j_{DC} \ln(j_{DC}/j_{min}), \quad (11)$$

which shows that smaller ramp rates, and better priming (larger j_{min}) result in smaller oscillations. It also shows that even moderate current peaks are being followed by a large current deeps.

If one takes into account dissipative processes in the external circuit or independent of the current sources of electrons, like exoemission or metastable-metastable collisions with production of electron-ion pairs (see [2, 7]), which result in the "energy" W loss over the oscillation period, then current oscillations will decay.

-
- [1] L.F. Weber, "Plasma Display Device Challenges," *Asia Display '98 Digest*, pp. 15-27, 1998.
L.F. Weber, "Plasma Panel Exhibiting Enhanced Contrast," *US Patent 5,745,086*, April 28, 1998.
- [2] V.P. Nagorny, P.J. Drallos and L.F. Weber, *SID'00 International Symposium Tech. Digest*, vol. XXXI, pp. 114-117, 2000.
- [3] J.K. Kim, J.H. Yang, W.J. Chung, K.W. Wang, "The addressing characteristics of an alternating current plasma display panel adopting a ramping reset pulse," *IEEE Transaction on Electron Devices*, vol. 48, pp. 1556-1563, 1995.
- [4] Yu.S. Akishev, et al., "Pulsed regime of the diffusive mode of a barrier discharge in helium," *Plasma Physics Reports*, vol. 27, pp. 164-171, 2001.
- [5] L. Mangolini et al., "Radial structure of a low-frequency atmospheric-pressure glow discharge in helium," *Appl. Phys. Letters*, vol. 80, pp. 1722-1724, 2002.
- [6] I. Radu, R. Bartnikas, and M.R. Wertheimer, "Frequency and voltage dependence of glow and pseudoglow discharges in helium under atmospheric pressure," *IEEE Transaction on Plasma Science*, vol. 31, pp. 1363-1378, 2003.
- [7] Yu B Golubovskii, et al., "Modelling of the homogeneous barrier discharge in helium at atmospheric pressure," *J. Phys. D: Appl. Phys.*, vol. 36, pp. 3949, 2003.
- [8] K. Sakita, et al., "High-speed address driving waveform analysis using wall voltage transfer function for three terminals and Vt Close Curve in three-electrode surface-discharge AC-PDPs," *SID'01 International Symposium Tech. Digest*, vol. XXXII, pp. 1022-1025, 2001.
- [9] H. Kim, et al., "Voltage domain analysis and wall voltage measurement for surface-discharge type ac-PDP," *SID'01 International Symposium Tech. Digest*, vol. XXXII, pp. 1026-1029, 2001.
- [10] V.P. Nagorny, P.J. Drallos and W. Williamson Jr., "The dynamics of a high-pressure ac gas discharge between dielectric coated electrodes near breakdown threshold," *J. Appl. Phys.*, vol. 77, pp. 3645-3656, 1995.
- [11] L. Oster, V. Yaskolko and J. Haddad, "Classification of exoelectron emission mechanisms," *Phys. Stat. Sol. A*, vol. 174, pp. 431-439, 1999.
- [12] L. Oster, V. Yaskolko and J. Haddad, "The experimental criteria for distinguishing different types of exoelectron emission mechanisms," *Phys. Stat. Sol. A*, vol. 187, pp. 481-485, 2001.
- [13] M. Molotskii, M. Naich and G. Rosenman, "Auger mechanism of exoelectron emission in dielectrics with high electron affinity," *J. Appl. Phys.*, vol. 94, pp. 4652-4658, 2003.
- [14] H. Tölner, "Exciting developments in plasma displays," *Proc. of IDW'04*, pp. 921-924, 2004.